

Bioanalytical Chemistry

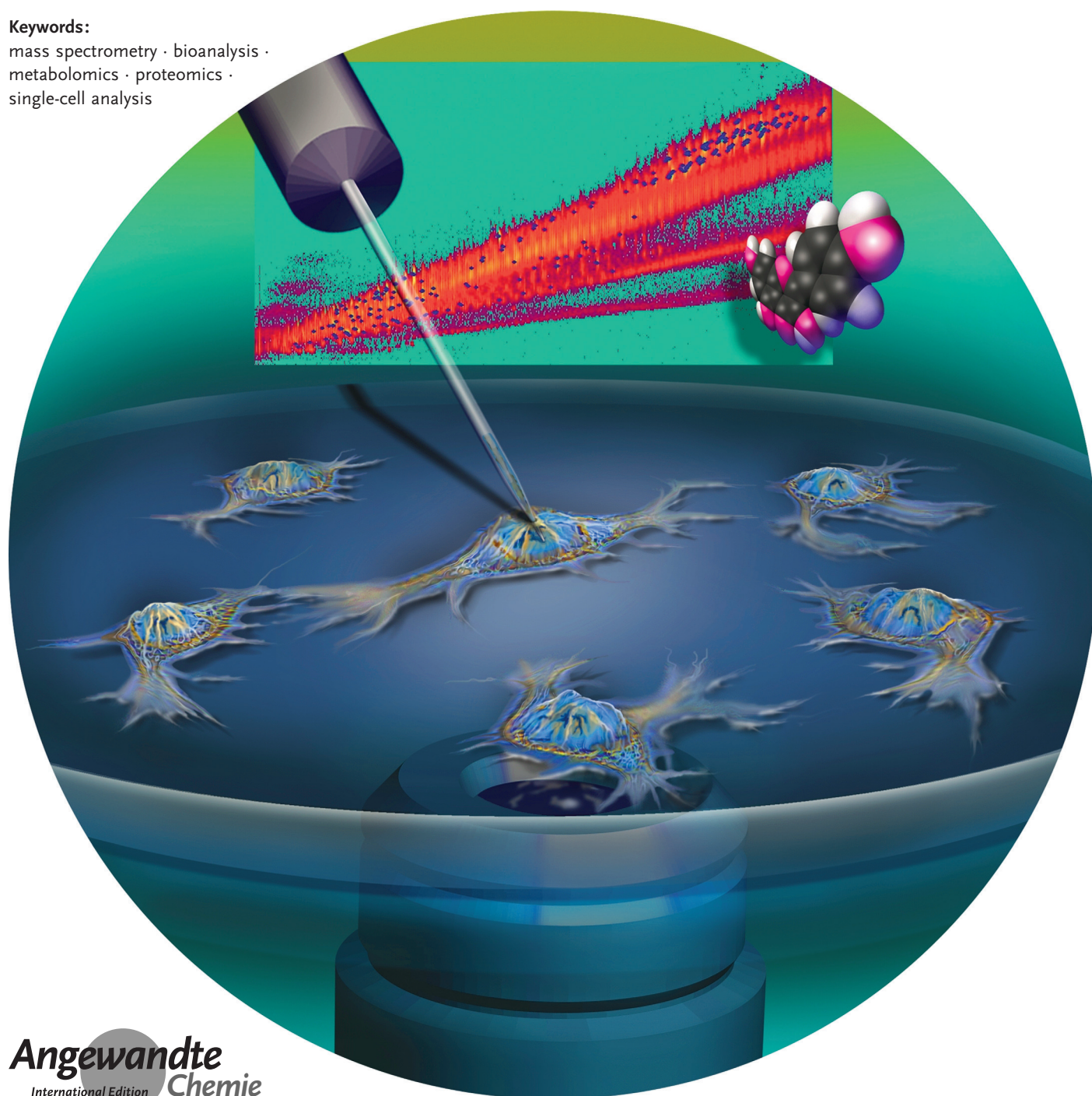
International Edition: DOI: 10.1002/anie.201709719
German Edition: DOI: 10.1002/ange.201709719

Single-Cell Mass Spectrometry Approaches to Explore Cellular Heterogeneity

Linwen Zhang and Akos Vertes*

Keywords:

mass spectrometry · bioanalysis ·
metabolomics · proteomics ·
single-cell analysis



Angewandte
International Edition
Chemie

4466 Wiley Online Library

© 2018 Wiley-VCH Verlag GmbH & Co. KGaA, Weinheim

Angew. Chem. Int. Ed. 2018, 57, 4466–4477

Compositional diversity is a fundamental property in cell populations. Single-cell analysis promises new insight into this cellular heterogeneity on the genomic, transcriptomic, proteomic, and metabolomic levels. Mass spectrometry (MS) is a label-free technique that enables the multiplexed analysis of proteins, peptides, lipids, and metabolites in individual cells. The abundances of these molecular classes are correlated with the physiological states and environmental responses of the cells. In this Minireview, we discuss recent advances in single-cell MS techniques with an emphasis on sampling and ionization methods developed for volume-limited samples. Strategies for sample treatment, separation methods, and data analysis require special considerations for single cells. Ongoing analytical challenges include subcellular heterogeneity, non-normal statistical distributions of cellular properties, and the need for high-throughput, high molecular coverage and minimal perturbation.

1. Introduction

Cellular heterogeneity, a phenomenon observed within a population of a given cell type, presents a major challenge in understanding how cells of a particular genotype function and respond to therapeutics.^[1] Some major causes for cellular heterogeneity are attributed to biochemical processes that are stochastic in nature, such as gene transcription and protein expression, functional differences, for example, stage in the cell cycle, and microenvironmental changes.^[2] To characterize these cell-to-cell differences and discern cellular subpopulations, molecular analysis at the single-cell level is necessary. The past two decades have seen an exponential growth in the field of “single-cell analysis”, as reflected by an increase in the use of this term in the literature from 249 in 1996 to 8,176 in 2016 (Web of Science, v 5.25).

Single-cell analysis techniques are being developed for all classes of biomolecules, including genes, transcripts, proteins, and metabolites. Owing to the power of DNA/RNA amplification technologies, gene^[3] and transcript^[4,5] analyses in single cells are well-established, whereas the corresponding untargeted proteomic and metabolomic methods are still in early development. Fluorescence techniques, primarily optical microscopy and flow cytometry, have been widely applied for the identification and quantitation of targeted proteins and metabolites in single cells.^[6–8] Other non-destructive approaches include Raman spectroscopy,^[9] electrochemistry,^[10] and microfluidics.^[11]

Table 1 shows reported data for volumes, absolute amounts of biomolecules, copy numbers per cell, and turnover times for transcripts, proteins and metabolites in single cells of *Escherichia coli*,^[12–18] *Saccharomyces cerevisiae*,^[13,17–22] *Arabidopsis thaliana*,^[23–29] and *Homo sapiens*.^[30–35] Decreasing cell volumes from plants (pL to low nL range), to animals (low pL range), to microbes (low fL range) present mounting difficulties for sample manipulation, and the correspondingly diminishing amounts of biomolecules re-

quire increasing sensitivities for detection and identification. Although for most species, the copy numbers per cell for transcripts are lower than for other biomolecules, the application of PCR amplification means that transcriptomics based on RNA sequencing (RNA-seq) in single cells is more advanced than other “omics” methods.

Untargeted detection and identification of proteins and metabolites typically rely on mass spectrometry (MS).^[36,37] This is a challenging undertaking due to the miniscule amounts of analytes in a cell (especially for proteins with low expression levels) and the wide range of copy numbers, sometimes spanning six orders of magnitude. Owing to the fast turnover rates of some biomolecules, rapid quenching and/or sampling steps are needed to preserve chemical compositions, in

particular for metabolites with turnover times on the millisecond timescale.^[38]

With high sensitivity and specificity, wide molecular coverage, relative quantitation, and structural identification capabilities, MS is becoming an important tool for single-cell proteomics and metabolomics. Recent advances in single-cell MS rely on improved instrumental performance with higher sensitivity and mass resolution, novel sampling and ionization approaches, and enhanced molecular coverage enabled by coupling MS with separation platforms, such as capillary electrophoresis (CE) or ion-mobility separation (IMS).

There is an inverse relationship between molecular coverage and spatial resolution on the one hand, and the analysis throughput on the other. For example, ion beams can be routinely focused to around 100 nm, whereas the spot size produced from laser beams typically exceeds the diffraction limit.^[39] Secondary-ion MS (SIMS) has been applied for imaging the subcellular distributions of metabolites, lipids, and pharmaceuticals.^[40–42] SIMS spectra, however, primarily contain information about low mass species ($m/z < 2000$). In contrast, matrix-assisted laser desorption/ionization (MALDI) MS^[43] and matrix-free laser desorption/ionization (LDI) MS,^[44,45] which have also been demonstrated for single-cell analysis, sample larger volumes and typically provide a larger molecular coverage. Similarly, low-throughput ambient ionization MS techniques allow chemical analysis with high molecular coverage,^[46] whereas mass cytometry is a high-throughput single-cell analysis method capable of distinguish-

[*] L. Zhang, Prof. A. Vertes
Department of Chemistry, The George Washington University
Washington, DC 20052 (USA)
E-mail: vertes@gwu.edu

 The ORCID identification number(s) for the author(s) of this article can be found under:
<https://doi.org/10.1002/anie.201709719>.

Table 1: Cell volumes (V), absolute amounts of biomolecules (m), copy numbers per cell (n), and turnover times (t_{to}) for transcripts, proteins, and metabolites in single cells of *E. coli*, *S. cerevisiae*, *A. thaliana*, and *H. sapiens*.

	V [pL]	Transcripts			Proteins			Metabolites		
		m [fmol]	n	t_{to} [s]	m [fmol]	n	t_{to} [s]	m [fmol]	n	t_{to} [s] ^[a]
<i>E. coli</i>	0.001	10^{-9} – 10^{-7}	1–100	60–1000	10^{-9} – 10^{-3}	1–300 000	60–200 000	10^{-7} –0.1	100 – 10^8	1–100
<i>S. cerevisiae</i>	0.03	10^{-9} – 10^{-7}	1–100	200–5000	10^{-8} – 10^{-3}	30 – 2×10^6	200–200 000	10^{-5} –1	$10\,000$ – 10^9	1–600
<i>A. thaliana</i> ^[b]	20	10^{-9} – 10^{-1}	1– 10^8	700–600 000	≤ 0.5	$\leq 3 \times 10^8$	30 000–100 000	2–10 000	10^9 – 7×10^{12}	0.3–100 000
<i>H. sapiens</i>	1	10^{-9} – 10^{-5}	1–4000	7000–90 000	10^{-7} – 10^{-1}	50 – 8×10^7	20 000–400 000	0.01–30	10^7 – 10^{10}	5–90 000

[a] Turnover rate ranges are presented for rapidly (ATP) and slowly (lysine) cycling metabolites. [b] Amounts and copy numbers are reported for RuBisCo (the most abundant plant protein).

ing a few dozen targeted analytes limited by the number of available metal tags.

Herein, we review the recent developments in single-cell MS propelled by new sampling and ionization strategies, with a focus on advances in micromanipulation, nanofabrication, and rapid gas-phase separation techniques, which also practiced in our laboratory. In order to obtain meaningful biological information, the highly dynamic nature of live cells has to be considered for proper sample handling. Unlike the analysis of large cell populations described by Gaussian statistics, the underlying distributions in single-cell analysis often follow non-normal distributions. The special considerations associated with sampling, ionization, sample preparation, and statistical data treatment in the analysis of individual cells are discussed in the following sections.

2. Single-Cell Proteomics and Metabolomics

There are two fundamentally different approaches for single-cell MS. With vacuum-based ion sources, the cells are often dehydrated and interrogated by an ion or laser beam for analysis. These ion sources provide excellent sensitivity and often high throughput for the analysis but the analyzed cells are far from their natural state due to the loss of water. In contrast, ambient ionization methods offer low perturbation for the cells, frequently under in situ or even in vivo conditions. These techniques, however, exhibit lower sensitivity, and in most cases low throughput. Historically, vacuum-based methods led the way to single-cell MS, so we start our discussion with these techniques.

2.1. Vacuum-Based Methods Offer High Sensitivity

Vacuum-based single-cell MS techniques historically encompass SIMS, MALDI, and matrix-free LDI methods. In the 1980s, early results for elemental transport in single cells were obtained by SIMS. With the development of nanoparticle matrixes in the 1990s, MALDI-MS also entered the single-cell analysis field. In the early 2000s, matrix-free LDI approaches were extended to tissues and individual cells. Each of these techniques can analyze tissue-embedded cells, and for isolated, floating, or circulating cells they can be combined with cell trapping and/or microscope-guided cell targeting methods.

With high surface sensitivity, and submicrometer lateral and nanometer depth resolution, time-of-flight (TOF) SIMS^[47] and nanoSIMS^[48,49] are often applied for the imaging of metabolites, lipids, pharmaceuticals, and their biotransformation products within single cells and subcellular compartments. In TOF-SIMS, this unique capability is based on a pulsed primary ion beam used to raster the sample surface with a spatial resolution of around 100 nm, and its accurate positioning with respect to the cell. An important advantage of SIMS imaging is that it collects morphological information in addition to molecular or elemental imaging. However, to maintain cellular shapes under high vacuum conditions, complex sample preparation steps, for example, the introduction of frozen hydrated samples, are required.^[50]

The introduction of cluster ion beams in SIMS has enabled imaging of the distributions of larger molecules on a subcellular scale with higher analyte ion yields.^[51–53] However, due to fragmentation and isobaric ion interferences introduced by the primary beam, conventional SIMS instru-



Linwen Zhang received her B.S. degree in pharmacy from China Pharmaceutical University in Nanjing, Jiangsu, China in 2011. She is currently a Ph.D. candidate under the guidance of Professor Akos Vertes at the Department of Chemistry of the George Washington University in Washington, DC, USA. Her research interests include the development and application of novel techniques based on mass spectrometry for the analysis of biological tissues, cells, and subcellular compartments.



Akos Vertes is a Professor of Chemistry and of Biochemistry and Molecular Biology at the George Washington University in Washington, DC, USA. He received his Ph.D. from the Eötvös Loránd University in Budapest, Hungary in 1979. His research interests encompass the development of new analytical techniques. Research areas include high-throughput methods in systems biology for rapid mechanism-of-action studies, new methods for molecular imaging of biological tissues under native conditions, and single-cell and subcellular analysis. He was elected Fellow of the U.S. National Academy of Inventors in 2013.

ments are limited in their identification capabilities. To overcome this issue, a new type of SIMS instrument has been designed to allow the fragmentation of selected precursor ions through collision-induced dissociation in parallel with conventional TOF-SIMS imaging.^[54]

A unique strength of SIMS imaging is its ability to capture molecular distributions in three dimensions with very high spatial and depth resolutions to enable subcellular studies. For example, the spatial and temporal distributions of lipid fragments on the surface of *Xenopus laevis* embryos during embryo cleavage were analyzed by TOF-SIMS 3D imaging.^[55] A recent 3D TOF-SIMS study showed subcellular distributions for the drug amiodarone and cellular metabolites in microphages.^[47] The drug was mainly observed on the surface and subsurface regions of the cells and was found absent in the nuclei. In other applications, 3D TOF-SIMS imaging was utilized to localize drugs and nanoparticles in subcellular regions.^[56,57]

A high-throughput single-cell analysis method was introduced by generating single-cell arrays with a micropatterned poly(dimethylsiloxane) stencil film followed by TOF-SIMS imaging.^[58] Drug-induced phenotypic changes in HeLa cells were studied with this technique. More recently, microscope-guided matrix-enhanced SIMS was developed for high-throughput analysis of diverse neurons.^[59] The coordinates of individual neurons were obtained by microscopic visualization and image processing, and the sample stage was moved according to the cell locations for matrix-enhanced SIMS analysis. This method allowed around 2000 cells to be analyzed in a single experiment.

With a capability for elemental and isotopic imaging at a lateral spatial resolution of around 50 nm, nanoSIMS has been applied for the quantitation of subcellular protein,^[60] DNA,^[48] lipid,^[61] neurotransmitter^[62] and drug^[63] distributions in single cells. To gain additional biological information, the molecular images by nanoSIMS are often correlated with the morphological information obtained by microscopy methods, for example, electron microscopy and super-resolution microscopy, and with electrochemical measurements.^[64] These methods have been thoroughly summarized in recent reviews.^[65,66]

With high-performance focusing optics that are capable of low micrometer or submicrometer spot sizes, MALDI-MS allows single-cell and subcellular analysis, respectively.^[67–69] This analysis can be conducted in the context of high-spatial-resolution MS imaging for tissue-embedded cells^[70,71] or local MS analysis for unicellular organisms^[72–74] and cells dissociated from tissues.^[75–77] In some cases, it is possible to use native cellular constituents as the matrix.^[78]

An important objective in single-cell analysis by MALDI-MS is to enhance the throughput. Microarrays for MS (MAMS), comprised of arrays of hydrophilic micro-wells patterned on an omniphobic surface, shows promise for the rapid analysis of up to 169 cells.^[73] A suspension of *S. cerevisiae* cells was deposited on the platform, and single or a few cells were trapped in each micro-well for MALDI-MS analysis. Metabolic variations between individual cells due to drug treatment or genetic modifications were explored, and phenotypic changes in metabolite levels were revealed. This

technique was also applied for the analysis of thousands of *Chlamydomonas reinhardtii* cells.^[74,79] More recently, this technique was combined with fluidic force microscopy (FluidFM) for the nondestructive and quantitative sampling of cell contents followed by MALDI-MS analysis (Figure 1).^[80] A cantilever probe, driven by an atomic force microscope, was used to gently extract 1 to 3 pL of the cytoplasm from HeLa cells and dispense it onto the MAMS substrate for MALDI-MS analysis. Another cell-trapping method, based on a micro-well patterned microfluidic chip, was introduced for the high-throughput analysis of phospholipids in single A549 cells by MALDI-MS imaging.^[81]

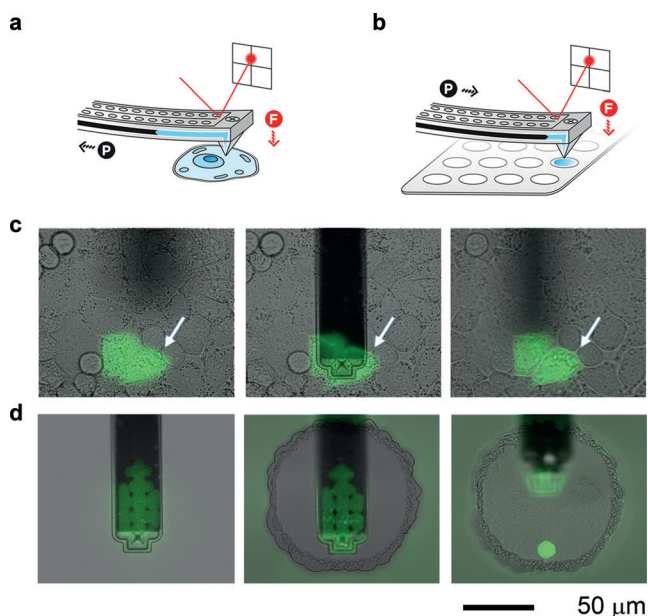


Figure 1. Microarrays for MS (MAMS) utilizes hydrophilic micro-wells to keep cytoplasm extracted from individual cells in place. Cell content is sampled by a fluidic force microscope (a) and redeposited into micro-wells for MALDI-MS analysis (b). Fluorescence imaging of GFP-labeled HeLa cells revealed efficient transfer of the cytoplasm during sampling (c) and redeposition (d). Adapted with permission from Ref. [80]. Copyright 2017 American Chemical Society.

Another high-throughput MALDI-MS approach utilized microscope imaging to identify the coordinates of individual cells dispersed on a microscope slide, and was used to analyze the peptide and protein species in targeted cells.^[75,76] Subpopulations and rare cells from hundreds to thousands of cells dissociated from mammalian organs (e.g., rat pituitary and pancreatic islets) were revealed by this technique. To expand metabolite coverage, single-cell MALDI-MS analysis of lipids and peptides was combined with microjunction extraction followed by CE-ESI-MS analysis of a broader class of small metabolites.^[82] Extracellular neuropeptides secreted from a single neuron were analyzed by combining solid-phase extraction and MALDI-MS (Figure 2).^[83]

To minimize spectral interference and ion suppression by the matrix in the low m/z range, several matrix-free LDI methods have been developed and applied for the analysis of small molecules in single cells. Nanostructure initiator MS

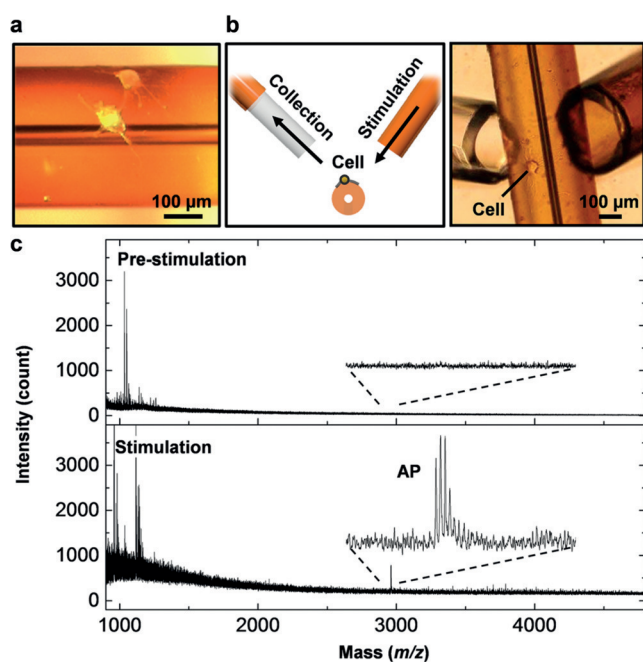


Figure 2. Analysis of neuropeptides excreted by a single neuron using solid-phase extraction and MALDI-MS detection. a) The neurons are attached to a polyimide capillary. b) They are stimulated with KCl solution and the excreted peptides are collected by solid-phase extraction. c) Mass spectra indicate the release of acidic peptide from a bag cell after stimulation. Reproduced with permission from Ref. [83] under Creative Commons Attribution 4.0 International License.

(NIMS) utilizes a heterogeneous structure composed of a nanoporous silicon substrate that can absorb the energy of the laser pulse, and an initiator compound trapped in the pores that contributes to the desorption and ionization of the sample.^[84] In an interesting application, NIMS was used to monitor metabolic changes and drug metabolism in single cells induced by chemotherapy.^[85]

Nanophotonic ionization relies on the interaction between the laser pulse and a nanostructure with dimensions commensurate with the wavelength of the light.^[86] The most studied examples, silicon nanopost array (NAPA) structures (Figure 3c), permit direct LDI-MS analysis of biological samples, including cell suspensions, adherent cells, and thin tissue sections, adhered or directly deposited on the NAPA surface.^[44,45,87] Through optimization of the post heights, diameters, and periodicities for maximum ion yields, a robust ultra-trace analysis platform was created with an LDI-MS limit of detection of around 800 zmol for verapamil.^[44,88,89] Single *S. cerevisiae* cells with a volume of around 30 fL were analyzed and 24 metabolites were tentatively identified.^[45] AFM images of a *S. cerevisiae* cell on NAPA before and after laser exposure are shown in Figure 3a,b.

To verify that NAPA-LDI-MS results on single yeast cells reflect biological changes, response to oxidative stress was studied. As expected from large population studies, upon exposure to hydrogen peroxide, the average reduced glutathione level (represented by ion intensities) in single *S. cerevisiae* cells was upregulated, and the distribution, reflecting cellular heterogeneity, showed a wider range (Figure 3d).

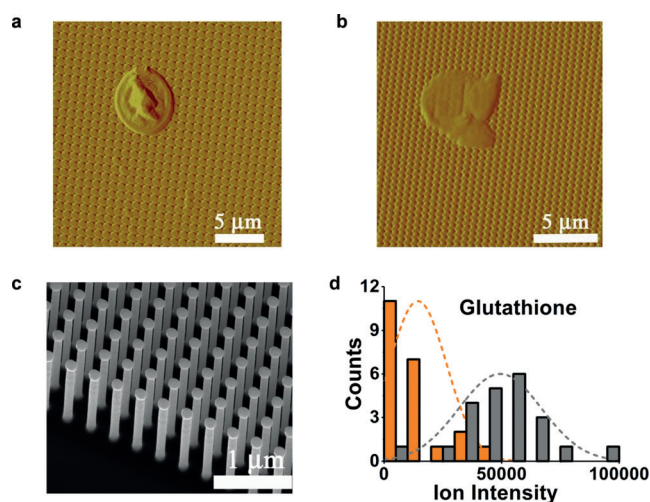


Figure 3. A single yeast cell imaged with AFM on top of a NAPA structure before (a) and after (b) laser exposure. c) SEM image of the NAPA chip before cell deposition. d) Distributions of glutathione abundances in cell populations raised in control (gray) and oxidative (orange) environments. Heterogeneity within the populations is shown by the width of the distribution, whereas differences in glutathione levels are represented by the mean values. Higher levels of glutathione, the main cellular redox buffer, are observed in cases of oxidative stress. Adapted from Ref. [45] with permission from John Wiley and Sons.

2.2. Ambient Ionization Methods Offer Low Perturbation

With the adaptation of recently introduced ambient ionization methods to single-cell MS, the analysis of live cells in their native environment became possible. This has major implications for single-cell analysis because of the significantly reduced mechanical and chemical perturbations and greatly simplified sample preparation. Minimizing perturbations is important because it helps to preserve metabolite, lipid, and peptide composition. Some metabolites have such high turnover rates that perturbations are reflected in their concentrations within milliseconds. Developments in ambient ionization MS techniques for single-cell analysis have recently been summarized in a thorough review.^[46] Here, we will focus on some of these technologies based on two types of sampling approaches, namely, probe sampling and laser ablation.

Live single-cell MS employs a metal-coated nanospray tip for cell sampling followed by ESI-MS analysis. It was applied to the metabolic analysis of single mammalian and plant cells.^[90–92] For example, this technique was applied to the identification and quantitation of plant hormones in single plant cells by introducing stable isotope-labeled standards in the electrospray solution.^[93] Recently, this technique was also applied to detect the localization of terpenoid indole alkaloids in specific cell types in *Catharanthus roseus* stems.^[94]

Capillary microsampling ESI-IMS-MS utilizes custom tailored capillaries and micromanipulators to extract 5–10% of the contents from cells of interest. The capillary containing the sample is used as a nanospray emitter to generate ions from the cell contents. The produced ions are separated based on their collision cross section (CCS) by IMS before mass analysis by a TOF analyzer. The IMS enables the separation

of isobaric ions and reduces the chemical background within milliseconds. This technique was applied to the analysis of metabolites and lipids for specific *A. thaliana* epidermal cells.^[95] Using IMS doubled the number of detected ionic species and enabled the tentative identification of 23 metabolites in individual cells. Comparing metabolite abundances in pavement and basal cells, and in trichomes, provided information on the presence of active metabolic pathways in these cellular phenotypes (Figure 4).

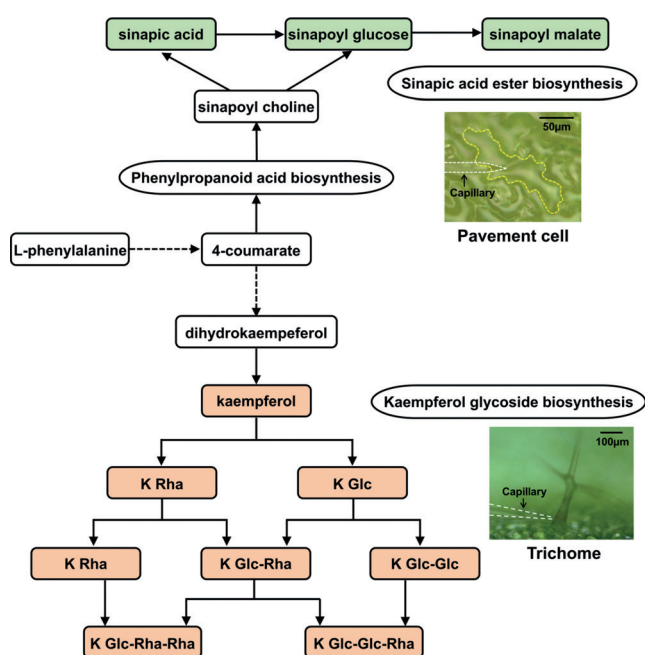


Figure 4. Capillary microsampling ESI-IMS-MS of *A. thaliana* epidermal cells reveals cell-type dependent activation of different metabolic pathways. In pavement and basal cells, sinapic acid ester biosynthesis is observed, whereas in trichomes, kaempferol glycoside biosynthesis is more prominent (K = kaempferol, Rha = rhamnoside and Glc = glucoside). Metabolites that are upregulated in pavement and basal cells, or in trichomes are shown with green and orange backgrounds, respectively. Adapted from Ref. [95] with permission from The Royal Society of Chemistry.

This technique was further applied to the metabolic and lipidomic analysis of smaller single cells, for example, human hepatocytes (Figure 5).^[96] Changes in metabolic heterogeneity over the distributions of cellular subpopulations were characterized in response to xenobiotic treatment. For example, a crucial molecular indicator of cell physiology, the adenylate energy charge, showed a dramatically altered distribution upon exposing the cells to rotenone, a known inhibitor of the electron transport chain in the mitochondria.

Another probe sampling method, single-probe MS, allows real-time cell sampling combined with nano-ESI-MS analysis.^[97] The single probe is a pulled double-barrel capillary, where one of the barrels is continuously supplied with electrospray solution and the other barrel is connected to a nanospray emitter. The single probe is inserted into the cell, and as the electrospray solution enters through one of the

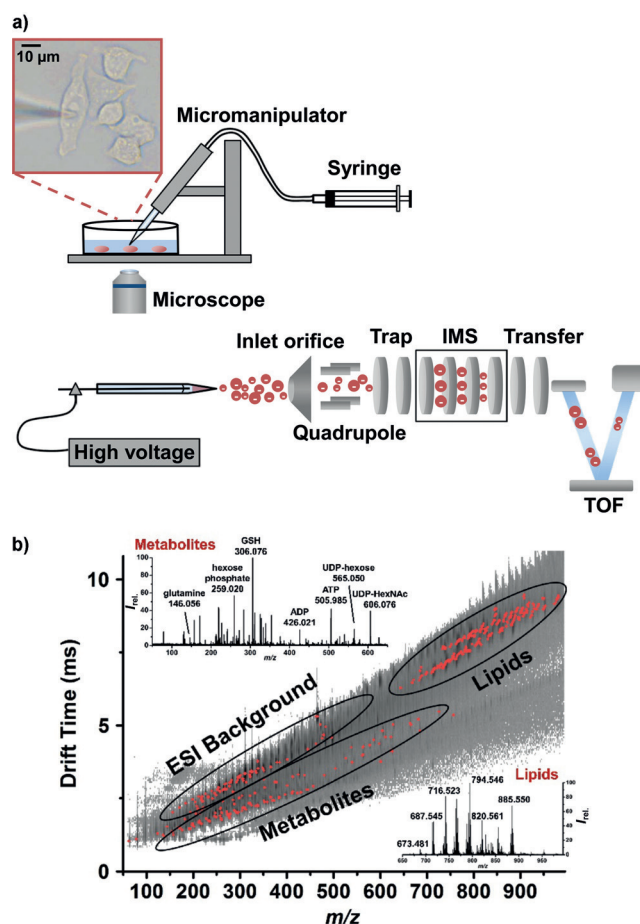


Figure 5. a) Capillary microsampling of a single human hepatocyte is followed by ESI-IMS-MS. b) The resulting DT versus m/z plot reveals efficient separation of small metabolites and lipids and the corresponding mass spectra (inset) show high signal-to-noise ratios. Adapted with permission from Ref. [96]. Copyright 2015 American Chemical Society.

barrels, the cell contents are extracted through the other one. This technique has been applied to the detection of adenylates, lipids, and drug molecules in individual HeLa cells treated with anticancer pharmaceuticals.^[97–98]

To simultaneously capture the metabolic and electrophysiological state of a neuron, the nano-ESI-MS method was combined with the patch-clamp technique.^[99] The unique combination of these two technologies enabled the identification of more than 50 metabolites in the cytoplasm of mouse brain neurons, and captured variations between different neuron types and mice of differing ages. Pairing electrophysiology with MS analysis for a single neuron presents great potential for molecular neuroscience.

Nanospray desorption electrospray ionization (nano-DESI) utilizes a primary capillary for solvent delivery on cell samples and a secondary capillary for picking up the extracted molecules for mass analysis. Recently, molecular imaging using this technique was applied to the metabolic and lipidomic analysis of a distribution of human cheek cells in a higher-throughput fashion.^[100]

Laser ablation based sampling methods for ambient single-cell MS mainly include laser ablation electrospray ionization (LAESI), laser desorption ionization droplet delivery (LDIDD), and atmospheric pressure MALDI (AP-MALDI) approaches. LAESI uses an etched optical fiber tip to deliver mid-IR laser pulses to individual cells for ablation and ESI for ionization of the ablation plume.^[101] This technique was first demonstrated for the analysis of individual epidermal cells and cell-by-cell imaging in plant bulb skins.^[101,102] Distinction of cell phenotypes and age was demonstrated based on the detection of 35 identified metabolites. For subcellular analysis, a single onion epidermal cell was dissected with a tungsten needle to expose the nucleus.^[103] The cytoplasm and nucleus were targeted separately by the fiber tip for LAESI-MS analysis, and differences in metabolic compositions were observed between the two subcellular compartments. More recently, this technique was applied for automated cell-by-cell imaging of the onion epidermis.^[104] Based on registering the cell centroids through the processing of microscope images, individual cells were presented to the fiber tip for ablation and ESI-MS analysis by an automated translation stage. This development opens the door for high-throughput cell-by-cell imaging.

In LDIDD-MS, an electrospray is directed to the sample surface, where individual cells are ablated by a pulsed UV laser. Charged secondary droplets produced by the electrospray are transferred to the mass spectrometer for analysis.^[105] Apoptosis and exocytosis in HEK cells was followed by this technique at the single-cell level. In a state-of-the-art AP-MALDI experiment, the combination of high numerical aperture focusing optics and optimized matrix deposition produced a spatial resolution of 1.4 μm . This resolution was sufficient to perform subcellular imaging of metabolites, lipids, and peptides in a single microbial cell.^[106]

2.3. Immunomarkers Offer High Selectivity

Mass cytometry is a high-throughput single-cell MS technique based on the combination of rare-earth elements tagged antibody labeling of the cells and inductively coupled plasma (ICP) MS analysis for the readout. This approach enables the simultaneous analysis of over 30 cellular features, for example, the presence of particular receptors, for millions of cells at a rate of around 2000 cells⁻¹.^[107] Unlike the overlapping spectra of fluorophores in flow cytometry, the rare-earth-element isotope signals can be clearly distinguish-

ed and quantified by ICP-MS (Figure 6).^[108] Mass cytometry represents a transition between targeted and untargeted methods, where fewer than 10 and more than 100 analytes, respectively, are identified. Recent advances in mass cytometry have been discussed in detail elsewhere.^[109–111] Here, we present some of the recent single-cell applications of this technique.

In one of its most powerful applications, mass cytometry was performed for the characterization of up to 28 surface markers of cells from bone marrow aspirates of leukemia patients and healthy individuals.^[112] In this comparative study, the expression levels of particular markers indicated cell biological properties, including immunophenotypes, cell-cycle stage, and intracellular signaling states, which were shown to be correlated with disease subtypes. High-throughput proteomics has rapidly expanded our knowledge of protein abundance levels in tissues and cells. Comparing the expression levels of mRNAs and the corresponding proteins in the same samples, however, showed only weak and varied correlation in multiple studies.^[113–115] One of the possible explanations of this unexpected finding is the cellular heterogeneity of the tissues and cell lines utilized in these investigations. To eliminate this possible source of bias, simultaneous quantitation of more than 40 transcripts and proteins from a single cell was recently made possible by mass cytometry combined with proximity ligation assay for mRNA.^[116] In this approach, two adjacent transcripts were hybridized with a pair of DNA oligonucleotide probes, which can be ligated and amplified, and further detected with metal-conjugated oligonucleotides in mass cytometry measurements. This technique was applied for the simultaneous quantitation of ten proteins and the corresponding transcripts in single primary human cells, and the results revealed that the levels of transcripts exhibited larger differences than proteins between individual cells.

The success of mass cytometry for circulating and suspended cells intensified efforts to extend this approach to tissue-embedded and adherent single cells. Recently, new variants of mass cytometry have been developed for tissue imaging with subcellular resolution.^[117] A high-resolution laser ablation system was combined with the labeling concept of mass cytometry for the imaging of proteins and their modifications at a spatial resolution of 1 μm in adherent cells and breast cancer tissue sections. Spatial distributions of cell heterogeneity in breast cancer tissue sections were identified within and between patients, thereby opening the door for the development of high-performance diagnostic tools.

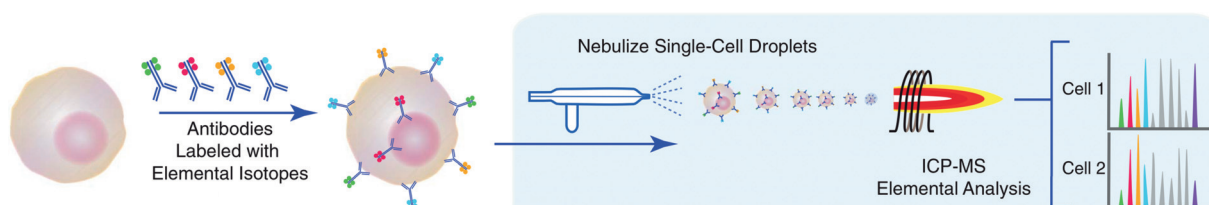


Figure 6. In mass cytometry, stable-isotope-labeled antibodies are used to tag cells expressing the corresponding antigens. Cells are nebulized into an inductively coupled plasma and elemental analysis by mass spectrometry reveals the tags associated with them. Adapted with permission from Ref. [108]. Copyright 2011 AAAS.

2.4. Hyphenated Methods Offer Enhanced Molecular Coverage

Increasing amounts of “omics” data indicate that an average single human cell can contain 10000 different types of proteins (not counting isoforms and posttranslational modifications)^[113] and more than 2500 metabolites. Even for macroscopic sample sizes, this degree of complexity cannot be resolved by MS alone. Integrating chemical separations with single-cell MS is needed to simplify mass spectra, minimize matrix effects, and enhance molecular identification confidence.

Microscale liquid chromatography (LC) and CE are prime candidates for combination with ESI-MS for single cells. In pioneering experiments, LC-ESI-MS was applied for quantitative single-cell analysis of close to 4000 proteins in *X. laevis* embryos.^[118,119] Likewise, combination of CE with ESI-MS enabled the metabolic analysis of single neurons from *Aplysia californica*.^[77,120] Recently, CE-ESI-MS has been adapted for single-cell metabolic (Figure 7) and proteomic analysis of low nanoliter samples from *X. laevis* embryos with a molecular coverage of 70 metabolites and 1709 protein groups.^[121–125]

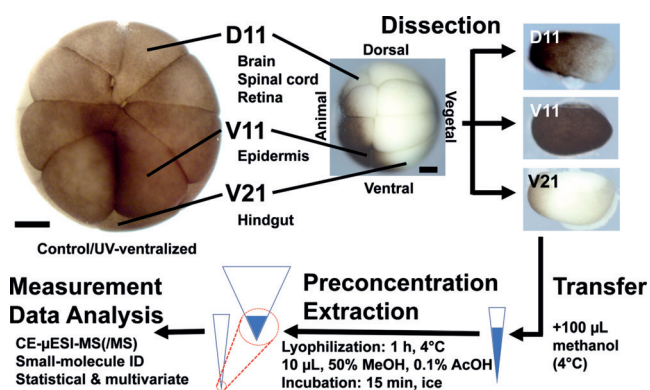


Figure 7. Cells from frog (*X. laevis*) embryos can be dissected and their contents analyzed by CE-ESI-MS for metabolites. (Scale bars: 250 µm.) Reproduced with permission from Ref. [121].

In comparison with the approaches mentioned above, IMS is a rapid separation technique that sorts ions based on their CCS on the millisecond timescale. As the separation takes place after ionization, IMS is compatible with direct sampling and ambient ionization methods. These attributes make this technique a choice candidate for single-cell analysis by MS. Single-cell ESI-IMS-MS has been shown to enhance molecular coverage, distinguish analytes from background interference, and separate isobaric ions in individual cells.^[95,96] In addition, there is a growing library of well-defined CCS values derived from IMS data that facilitates the identification of cellular metabolites and lipids.^[96] However, the relatively low drift time resolving power ($R < 100$) of the current commercially available IMS systems presents a limitation. Newly developed high-resolution IMS instruments ($R > 250$)^[126] raise the prospect of distinguishing structural isomers in single-cell MS.

3. Mitigating Perturbations Due to Sampling

Cells rapidly respond to environmental stress by changing their molecular composition. Stressors include molecular and ionic changes in the environment, altered temperature, and sustained or strong mechanical forces. Therefore, the objective of sample preparation is to minimize the perturbation exerted on the cells by the analytical process. In plant and animal cells, the fastest turnover times for transcripts and proteins are in excess of 10 min (see Table 1). Metabolites and peptides, however, can exhibit turnover times of around 1 s. To prevent metabolite and peptide degradation during single-cell measurements, the biochemical processes are quenched, typically by denaturing the enzymes, for example, through rapid cooling, heating, or acidification. In addition, specific sample treatment steps are required for the different MS techniques. For vacuum-based techniques, cell membrane shape and molecular compositions need to be preserved under high-vacuum conditions. For example, chemical fixation or freeze-drying of cell samples is performed for SIMS-MS.^[39,127] For MS of live cells under ambient conditions, close to physiological conditions can be maintained throughout most of the measurement. Ideally, cultured cells are placed in a buffer solution or medium in a humidity- and temperature-controlled chamber during sampling, and immediately subjected to MS analysis.

To minimize stress, the selection of optimal cell sampling and isolation methods are also critical. Laser capture microdissection can be applied to isolate individual cells of interest from heterogeneous tissue samples.^[128] However, molecular changes potentially induced by the physical isolation and preparation needed for this technique have to be kept at a minimum. Live-cell sampling in LAESI occurs on the millisecond timescale under ambient conditions, thereby maintaining the cells in their native state until right before analysis.^[101,102,104] Recent advances offered by microfluidic cell isolation, capture, and lysis coupled with MS result in enhanced analytical throughput but also exert shear stress on the cells.^[129] In situ sampling with probes, such as capillary microsampling, enables direct extraction of cell contents.^[95–96] However, cell membrane rupture by the capillary tip during sampling can induce mechanical stress, and sampling bias with respect to the inclusion of small organelles might exist. Rapid sampling and MS measurements are necessary to minimize the degradation of cellular metabolites and lipids. To enhance the experimental throughput and reproducibility, robotic capillary microsampling or automated laser ablation can be explored. For example, automated patch clamping controlled by a robot has been introduced to target individual neurons of interest and measure their electrophysiological conditions.^[130–131] This approach can be combined with capillary microsampling followed by ESI-MS analysis in a rapid and controlled fashion.

4. Skewed Distributions: What's in the Noise?

Compared to bulk measurements, single-cell data often follow non-normal distributions, and the analysis requires

special considerations. This challenge stems from the convolution of biological and technical noise, the common presence of non-normal copy-number distributions over the studied cell populations, the typically low signal-to-noise ratios with the presence of dropout events at low abundance, and the existence of subpopulations. The analysis methods required for such data have been developed for single-cell RNA-seq, and many of them can be adapted for single-cell MS.

Technical noise is the unavoidable fluctuation of the signal resulting from the analytical method itself. Technical noise in RNA-seq was shown to increase as the sample amounts were reduced.^[132] Similarly, the technical noise is more significant for molecular components of lower abundance within a sample. To reveal biological variability, the technical noise needs to be determined for each component separately, and at the biological abundance levels. In single-cell RNA-seq experiments, the technical noise was characterized by measuring the signal fluctuations for spiked-in gene products that covered the entire dynamic range of interest.^[132] In single-cell metabolomics by MS, technical noise was evaluated for a few components using a similar strategy.^[96] For a particular molecular species, the technical noise was characterized by microsampling homogenous solutions with cellular concentrations. For largescale studies, mixtures of chemical standards or their isotopologues can be measured at physiological concentrations and under conditions identical to the single-cell experiments. Once the technical noise is determined, it can be deconvoluted from the single-cell data to find the biological variability.

Molecular copy numbers in a cell population can exhibit normal or non-normal skewed profiles, sometimes with long tails. Under environmental stress, the median and the shape of the distribution can be shifted and distorted, respectively. Pronounced changes in the molecular noise may indicate that a chemical species is involved in pathways significantly affected by the perturbations. The distribution of a molecular species and the corresponding error model have to be determined before the appropriate statistical method can be selected. For a non-normal distribution, data points that appear to be statistical outliers may represent biological information for the rare cells. These data points require special attention instead of being discarded as outliers. For example, dropout events in an RNA-seq experiment were captured by a Poisson distribution, whereas proper amplification was described by a negative binomial component.^[133] The resulting error model enhanced the robustness of subpopulation detection.

System-wide analysis of transcripts and proteins in bacteria revealed that the corresponding copy numbers followed gamma distributions.^[134] Depending on the protein copy numbers per cell, the corresponding noise levels approached two limiting behaviors. For low copy numbers ($n < 10$), the noise levels were inversely proportional to the mean copy number $\langle n \rangle$, whereas for large copy numbers the noise was limited by a constant noise level. Establishing biological noise behavior for proteins through fluorescence methods is essential for the interpretation of emerging single-cell protein MS data.

5. New Frontiers

During the past decade, novel single-cell MS techniques have emerged for the multiplexed analysis of intracellular molecules, including metabolites, lipids, peptides, and proteins. Beyond providing qualitative information on the presence of these molecular species, single-cell MS also offers quantitative data, thereby enabling the characterization of cellular heterogeneity and the identification of subpopulations.

Since single-cell MS is still in its early development, several challenges remain. First, although the throughput of some single-cell MS techniques, such as mass cytometry and MALDI-MS, has greatly improved, other methods are still painfully slow. The high-throughput approaches do not cover certain important applications, for example, the non-targeted analysis of tissue-embedded cells. For these sample types, high-throughput analysis of more than 1000 cells has not yet been achieved. The proliferation of robotic sampling approaches is anticipated to circumvent the slow manual selection and isolation of single cells.

Most of the current single-cell MS techniques are destructive, which limits the analysis of temporal changes in a cell during development or under drug treatment. This impediment can be alleviated by developing minimally destructive sampling methods and improving the instrumental sensitivity to detect ever decreasing amounts of cell content.

To achieve multifaceted analysis capturing additional cellular properties and obtain more dynamic information, single-cell MS can be coupled with other analytical tools to explore cell behavior and specific subpopulations. These techniques are based on non-destructive approaches that allow subsequent MS analysis. They include patch-clamp experiments,^[135] fluorescence microscopy,^[7,8] and Raman spectroscopy.^[9]

The availability of high-throughput cell sorting and single-cell RNA-seq combined with the emerging single-cell proteomics and metabolomics methods raises the prospect of single-cell systems biology. Since the studied cells come from a well-defined subpopulation, the underlying biological pathways are better defined and the corresponding bioinformatics can be simplified.

Despite the technical challenges faced by single-cell MS, it promises new insight into cell biology and biochemistry that cannot be gained through bulk analysis methods. Joined with single-cell RNA-seq, we expect single-cell MS to become a useful tool for rapid disease diagnostics in clinical applications.

Acknowledgements

Research was sponsored by the U.S. Army Research Office and the Defense Advanced Research Projects Agency and was accomplished under cooperative agreement number W911NF-14-2-0020. The views and conclusions contained in this document are those of the authors and should not be interpreted as representing the official policies, either ex-

pressed or implied, of the Army Research Office, DARPA, or the U.S. Government. The U.S. Government is authorized to reproduce and distribute reprints for Government purposes notwithstanding any copyright notation hereon.

Conflict of interest

The authors declare no conflict of interest.

How to cite: *Angew. Chem. Int. Ed.* **2018**, *57*, 4466–4477
Angew. Chem. **2018**, *130*, 4554–4566

-
- [1] S. J. Altschuler, L. F. Wu, *Cell* **2010**, *141*, 559–563.
- [2] A. Raj, A. van Oudenaarden, *Cell* **2008**, *135*, 216–226.
- [3] P. Eirew, A. Steif, J. Khattri, G. Ha, D. Yap, H. Farahani, K. Gelmon, S. Chia, C. Mar, A. Wan, E. Laks, J. Biele, K. Shumansky, J. Rosner, A. McPherson, C. Nielsen, A. J. L. Roth, C. Lefebvre, A. Bashashati, C. de Souza, C. Siu, R. Aniba, J. Brimhall, A. Oloumi, T. Osako, A. Bruna, J. L. Sandoval, T. Algara, W. Greenwood, K. Leung, H. W. Cheng, H. Xue, Y. Z. Wang, D. Lin, A. J. Mungall, R. Moore, Y. J. Zhao, J. Lorette, L. Nguyen, D. Huntsman, C. J. Eaves, C. Hansen, M. A. Marra, C. Caldas, S. P. Shah, S. Aparicio, *Nature* **2015**, *518*, 422–426.
- [4] I. Tirosh, A. S. Venteicher, C. Hebert, L. E. Escalante, A. P. Patel, K. Yizhak, J. M. Fisher, C. Rodman, C. Mount, M. G. Filbin, C. Neftel, N. Desai, J. Nyman, B. Izar, C. C. Luo, J. M. Francis, A. A. Patel, M. L. Onozato, N. Riggi, K. J. Livak, D. Gennert, R. Satija, B. V. Nahed, W. T. Curry, R. L. Martuza, R. Mylvaganam, A. J. Iafrate, M. P. Frosch, T. R. Golub, M. N. Rivera, G. Getz, O. Rozenblatt-Rosen, D. P. Cahill, M. Monje, B. E. Bernstein, D. N. Louis, A. Regev, M. L. Suva, *Nature* **2016**, *539*, 309–313.
- [5] A. C. Villani, R. Satija, G. Reynolds, S. Sarkizova, K. Shekhar, J. Fletcher, M. Griesbeck, A. Butler, S. W. Zheng, S. Lazo, L. Jardine, D. Dixon, E. Stephenson, E. Nilsson, I. Grundberg, D. McDonald, A. Filby, W. B. Li, P. L. De Jager, O. Rozenblatt-Rosen, A. A. Lane, M. Haniffa, A. Regev, N. Hacohen, *Science* **2017**, *356*, eaah4573.
- [6] N. Baumgarth, M. Roederer, *J. Immunol. Methods* **2000**, *243*, 77–97.
- [7] Q. L. Li, P. L. Chen, Y. Y. Fan, X. Wang, K. H. Xu, L. Li, B. Tang, *Anal. Chem.* **2016**, *88*, 8610–8616.
- [8] M. Mondal, R. J. Liao, L. Xiao, T. Eno, J. Guo, *Angew. Chem. Int. Ed.* **2017**, *56*, 2636–2639; *Angew. Chem.* **2017**, *129*, 2680–2683.
- [9] R. Smith, K. L. Wright, L. Ashton, *Analyst* **2016**, *141*, 3590–3600.
- [10] X. C. Li, S. Majdi, J. Dunevall, H. Fathali, A. G. Ewing, *Angew. Chem. Int. Ed.* **2015**, *54*, 11978–11982; *Angew. Chem.* **2015**, *127*, 12146–12150.
- [11] B. L. Wang, A. Ghaderi, H. Zhou, J. Agresti, D. A. Weitz, G. R. Fink, G. Stephanopoulos, *Nat. Biotechnol.* **2014**, *32*, 473–478.
- [12] R. Milo, R. Phillips, *Cell Biology by the Numbers*, Garland Science, New York, **2016**.
- [13] P. Lu, C. Vogel, R. Wang, X. Yao, E. M. Marcotte, *Nat. Biotechnol.* **2007**, *25*, 117–124.
- [14] J. A. Bernstein, A. B. Khodursky, P. H. Lin, S. Lin-Chao, S. N. Cohen, *Proc. Natl. Acad. Sci. USA* **2002**, *99*, 9697–9702.
- [15] B. Soufi, K. Krug, A. Harst, B. Macek, *Front. Microbiol.* **2015**, *6*, 103.
- [16] M. R. Maurizi, *Experientia* **1992**, *48*, 178–201.
- [17] J. O. Park, S. A. Rubin, Y. F. Xu, D. Amador-Noguez, J. Fan, T. Shlomi, J. D. Rabinowitz, *Nat. Chem. Biol.* **2016**, *12*, 482–489.
- [18] J. J. Heijnen in *Biosystems Engineering II: Linking Cellular Networks and Bioprocesses, Vol. 121* (Eds.: C. Wittmann, R. Krull), Springer-Verlag, Berlin, **2010**, pp. 139–162.
- [19] I. Soifer, N. Barkai, *Mol. Syst. Biol.* **2014**, *10*, 761.
- [20] N. A. Kulak, G. Pichler, I. Paron, N. Nagaraj, M. Mann, *Nat. Methods* **2014**, *11*, 319–324.
- [21] Y. L. Wang, C. L. Liu, J. D. Storey, R. J. Tibshirani, D. Herschlag, P. O. Brown, *Proc. Natl. Acad. Sci. USA* **2002**, *99*, 5860–5865.
- [22] A. Belle, A. Tanay, L. Bitincka, R. Shamir, E. K. O'Shea, *Proc. Natl. Acad. Sci. USA* **2006**, *103*, 13004–13009.
- [23] G. Gutierrez-Alcala, C. Gotor, A. J. Meyer, M. Fricker, J. M. Vega, L. C. Romero, *Proc. Natl. Acad. Sci. USA* **2000**, *97*, 11108–11113.
- [24] H. Shimada, T. Obayashi, N. Takahashi, M. Matsui, A. Sakamoto, *Plant Methods* **2010**, *6*, 29.
- [25] R. Narsai, K. A. Howell, A. H. Millar, N. O'Toole, I. Small, J. Whelan, *Plant Cell* **2007**, *19*, 3418–3436.
- [26] L. Li, C. J. Nelson, J. Trosch, I. Castleden, S. B. Huang, A. H. Millar, *Plant Cell* **2017**, *29*, 207–228.
- [27] S. Arrivault, M. Guenther, A. Ivakov, R. Feil, D. Vosloh, J. T. van Dongen, R. Sulpice, M. Stitt, *Plant J.* **2009**, *59*, 826–839.
- [28] S. Sato, S. Yanagisawa, *Plant Cell Physiol.* **2014**, *55*, 306–319.
- [29] X. Y. Yang, W. P. Chen, A. K. Rendahl, A. D. Hegeman, W. M. Gray, J. D. Cohen, *Plant J.* **2010**, *63*, 680–695.
- [30] J. R. Wisniewski, A. Vildhede, A. Noren, P. Artursson, *J. Proteomics* **2016**, *136*, 234–247.
- [31] S. Wilkening, F. Stahl, A. Bader, *Drug Metab. Dispos.* **2003**, *31*, 1035–1042.
- [32] H. Tani, R. Mizutani, K. A. Salam, K. Tano, K. Ijiri, A. Wakamatsu, T. Isogai, Y. Suzuki, N. Akimitsu, *Genome Res.* **2012**, *22*, 1382.
- [33] S. B. Cambridge, F. Gnad, C. Nguyen, J. L. Bermejo, M. Kruger, M. Mann, *J. Proteome Res.* **2011**, *10*, 5275–5284.
- [34] L. F. Barros, A. San Martin, T. Sotelo-Hitschfeld, R. Lerchundi, I. Fernandez-Moncada, I. Ruminot, R. Gutierrez, R. Valdebenito, S. Ceballo, K. Alegria, F. Baeza-Lehnert, D. Espinoza, *Front. Cell. Neurosci.* **2013**, *7*, 27.
- [35] P. Righetti, E. P. Little, G. Wolf, *J. Biol. Chem.* **1971**, *246*, 5724–5732.
- [36] A. Svatos, *Anal. Chem.* **2011**, *83*, 5037–5044.
- [37] T. J. Comi, T. D. Do, S. S. Rubakhin, J. V. Sweedler, *J. Am. Chem. Soc.* **2017**, *139*, 3920–3929.
- [38] R. Zenobi, *Science* **2013**, *342*, 1243259.
- [39] E. J. Lanni, S. S. Rubakhin, J. V. Sweedler, *J. Proteomics* **2012**, *75*, 5036–5051.
- [40] M. E. Kurczy, P. D. Pichowski, C. T. Van Bell, M. L. Heien, N. Winograd, A. G. Ewing, *Proc. Natl. Acad. Sci. USA* **2010**, *107*, 2751–2756.
- [41] S. G. Ostrowski, C. T. Van Bell, N. Winograd, A. G. Ewing, *Science* **2004**, *305*, 71–73.
- [42] D. R. Smith, S. Chandra, R. F. Barth, W. L. Yang, D. D. Joel, J. A. Coderre, *Cancer Res.* **2001**, *61*, 8179–8187.
- [43] B. Spengler, M. Hubert, *J. Am. Soc. Mass Spectrom.* **2002**, *13*, 735–748.
- [44] B. N. Walker, J. A. Stolee, A. Vertes, *Anal. Chem.* **2012**, *84*, 7756–7762.
- [45] B. N. Walker, C. Antonakos, S. T. Retterer, A. Vertes, *Angew. Chem. Int. Ed.* **2013**, *52*, 3650–3653; *Angew. Chem.* **2013**, *125*, 3738–3741.
- [46] Y. Yang, Y. Huang, J. Wu, N. Liu, J. Deng, T. Luan, *Trac-Trends Anal. Chem.* **2017**, *90*, 14–26.
- [47] M. K. Passarelli, C. F. Newman, P. S. Marshall, A. West, I. S. Gilmore, J. Bunch, M. R. Alexander, C. T. Dollery, *Anal. Chem.* **2015**, *87*, 6696–6702.

- [48] M. L. Steinhäuser, A. P. Bailey, S. E. Senyo, C. Guillemer, T. S. Perlstein, A. P. Gould, R. T. Lee, C. P. Lechene, *Nature* **2012**, *481*, 516–519.
- [49] N. Musat, R. Foster, T. Vagner, B. Adam, M. M. M. Kuypers, *FEMS Microbiol. Rev.* **2012**, *36*, 486–511.
- [50] N. Winograd, A. Bloom in *Mass Spectrometry Imaging of Small Molecules, Vol. 1203* (Ed.: L. He), Humana Press, New York, **2015**, pp. 9–19.
- [51] D. Breitenstein, C. E. Rommel, R. Mollers, J. Wegener, B. Hagenhoff, *Angew. Chem. Int. Ed.* **2007**, *46*, 5332–5335; *Angew. Chem.* **2007**, *119*, 5427–5431.
- [52] H. Nygren, B. Hagenhoff, P. Malmberg, M. Nilsson, K. Richter, *Microsc. Res. Tech.* **2007**, *70*, 969–974.
- [53] H. Jungnickel, P. Laux, A. Luch, *Toxics* **2016**, *4*, 5.
- [54] G. L. Fisher, A. L. Bruinen, N. O. Potocnik, J. S. Hammond, S. R. Bryan, P. E. Larson, R. M. A. Heeren, *Anal. Chem.* **2016**, *88*, 6433–6440.
- [55] H. Tian, J. S. Fletcher, R. Thuret, A. Henderson, N. Papalopulu, J. C. Vickerman, N. P. Lockyer, *J. Lipid Res.* **2014**, *55*, 1970–1980.
- [56] Q. P. Vanbellingen, A. Castellanos, M. Rodriguez-Silva, I. Paudel, J. W. Chambers, F. A. Fernandez-Lima, *J. Am. Soc. Mass Spectrom.* **2016**, *27*, 2033–2040.
- [57] D. J. Graham, J. T. Wilson, J. J. Lai, P. S. Stayton, D. G. Castner, *Biointerphases* **2016**, *11*, 02A304.
- [58] L. Huang, Y. Chen, L. T. Weng, M. Leung, X. X. Xing, Z. Y. Fan, H. K. Wu, *Anal. Chem.* **2016**, *88*, 12196–12203.
- [59] T. D. Do, T. J. Comi, S. J. B. Dunham, S. S. Rubakhin, J. V. Sweedler, *Anal. Chem.* **2017**, *89*, 3078–3086.
- [60] I. C. Vreja, S. Kabatas, S. K. Saka, K. Krohnert, C. Hoschen, F. Opazo, U. Diederichsen, S. O. Rizzoli, *Angew. Chem. Int. Ed.* **2015**, *54*, 5784–5788; *Angew. Chem.* **2015**, *127*, 5876–5880.
- [61] H. B. Jiang, C. N. Goulbourne, A. Tatar, K. Turlo, D. Wu, A. P. Beigneux, C. R. M. Grovenor, L. G. Fong, S. G. Young, *J. Lipid Res.* **2014**, *55*, 2156–2166.
- [62] J. Lovric, J. Dunevall, A. Larsson, L. Ren, S. Andersson, A. Meibom, P. Malmberg, M. E. Kurczyk, A. G. Ewing, *ACS Nano* **2017**, *11*, 3446–3455.
- [63] H. B. Jiang, M. K. Passarelli, P. M. G. Munro, M. R. Kilburn, A. West, C. T. Dollery, I. S. Gilmore, P. D. Rakowska, *Chem. Commun.* **2017**, *53*, 1506–1509.
- [64] N. T. N. Phan, X. C. Li, A. G. Ewing, *Nat. Rev. Chem.* **2017**, *1*, 0048.
- [65] H. B. Jiang, M. R. Kilburn, J. Decelle, N. Musat, *Curr. Opin. Biotechnol.* **2016**, *41*, 130–135.
- [66] K. N. Richter, S. O. Rizzoli, S. Jahne, A. Vogts, J. Lovric, *Neurophotonics* **2017**, *4*, 020901.
- [67] K. J. Boggio, E. Obasuyi, K. Sugino, S. B. Nelson, N. Y. R. Agar, J. N. Agar, *Expert Rev. Proteomics* **2011**, *8*, 591–604.
- [68] A. Zavalin, E. M. Todd, P. D. Rawhouser, J. H. Yang, J. L. Norris, R. M. Caprioli, *J. Mass Spectrom.* **2012**, *47*, 1473–1481.
- [69] G. Thiery-Lavenant, A. I. Zavalin, R. M. Caprioli, *J. Am. Soc. Mass Spectrom.* **2013**, *24*, 609–614.
- [70] R. M. Caprioli, *Proteomics* **2016**, *16*, 1607–1612.
- [71] Y. Schober, S. Guenther, B. Spengler, A. Rompp, *Anal. Chem.* **2012**, *84*, 6293–6297.
- [72] P. L. Urban, K. Jefimovs, A. Amantonico, S. R. Fagerer, T. Schmid, S. Madler, J. Puigmarti-Luis, N. Goedecke, R. Zenobi, *Lab Chip* **2010**, *10*, 3206–3209.
- [73] A. J. Ibanez, S. R. Fagerer, A. M. Schmidt, P. L. Urban, K. Jefimovs, P. Geiger, R. Dechant, M. Heinemann, R. Zenobi, *Proc. Natl. Acad. Sci. USA* **2013**, *110*, 8790–8794.
- [74] J. Krismer, J. Sobek, R. F. Steinhoff, S. R. Fagerer, M. Pabst, R. Zenobi, *Appl. Environ. Microbiol.* **2015**, *81*, 5546–5551.
- [75] T. H. Ong, D. J. Kissick, E. T. Jansson, T. J. Comi, E. V. Romanova, S. S. Rubakhin, J. V. Sweedler, *Anal. Chem.* **2015**, *87*, 7036–7042.
- [76] E. T. Jansson, T. J. Comi, S. S. Rubakhin, J. V. Sweedler, *ACS Chem. Biol.* **2016**, *11*, 2588–2595.
- [77] P. Nemes, A. M. Knolhoff, S. S. Rubakhin, J. V. Sweedler, *ACS Chem. Neurosci.* **2012**, *3*, 782–792.
- [78] T. Jaschinski, E. J. N. Helfrich, C. Bock, S. Wolfram, A. Svatos, C. Hertweck, G. Pohnert, *J. Mass Spectrom.* **2014**, *49*, 136–144.
- [79] J. Krismer, M. Tamminen, S. Fontana, R. Zenobi, A. Narwani, *ISME J.* **2017**, *11*, 988–998.
- [80] O. Guillaume-Gentil, T. Rey, P. Kiefer, A. J. Ibanez, R. Steinhoff, R. Bronnimann, L. Dorwling-Carter, T. Zambelli, R. Zenobi, J. A. Vorholt, *Anal. Chem.* **2017**, *89*, 5017–5023.
- [81] W. Y. Xie, D. Gao, F. Jin, Y. Y. Jiang, H. X. Liu, *Anal. Chem.* **2015**, *87*, 7052–7059.
- [82] T. J. Comi, M. A. Makurath, M. C. Philip, S. S. Rubakhin, J. V. Sweedler, *Anal. Chem.* **2017**, *89*, 7765–7772.
- [83] C. Y. Lee, Y. Fan, S. S. Rubakhin, S. Yoon, J. V. Sweedler, *Sci. Rep.* **2016**, *6*, 26940.
- [84] T. R. Northen, O. Yanes, M. T. Northen, D. Marrinucci, W. Uritboonthai, J. Apon, S. L. Golledge, A. Nordstrom, G. Siuzdak, *Nature* **2007**, *449*, 1033–1036.
- [85] P. J. O'Brien, M. Lee, M. E. Spilker, C. C. Zhang, Z. Yan, T. C. Nichols, W. Li, C. H. Johnson, G. J. Patti, G. Siuzdak, *Cancer Metabolism* **2013**, *1*, 4.
- [86] J. A. Stolee, B. N. Walker, V. Zorba, R. E. Russo, A. Vertes, *Phys. Chem. Chem. Phys.* **2012**, *14*, 8453–8471.
- [87] S. A. Stopka, C. Rong, A. R. Korte, S. Yadavilli, J. Nazarian, T. T. Razunguzwa, N. J. Morris, A. Vertes, *Angew. Chem. Int. Ed.* **2016**, *55*, 4482–4486; *Angew. Chem.* **2016**, *128*, 4558–4562.
- [88] B. N. Walker, J. A. Stolee, D. L. Pickel, S. T. Retterer, A. Vertes, *Appl. Phys. A* **2010**, *101*, 539–544.
- [89] B. N. Walker, J. A. Stolee, D. L. Pickel, S. T. Retterer, A. Vertes, *J. Phys. Chem. C* **2010**, *114*, 4835–4840.
- [90] H. Mizuno, N. Tsuyama, T. Harada, T. Masujima, *J. Mass Spectrom.* **2008**, *43*, 1692–1700.
- [91] T. Masujima, *Anal. Sci.* **2009**, *25*, 953–960.
- [92] T. Fujii, S. Matsuda, M. L. Tejedor, T. Esaki, I. Sakane, H. Mizuno, N. Tsuyama, T. Masujima, *Nat. Protoc.* **2015**, *10*, 1445–1456.
- [93] T. Shimizu, S. Miyakawa, T. Esaki, H. Mizuno, T. Masujima, T. Koshiba, M. Seo, *Plant Cell Physiol.* **2015**, *56*, 1287–1296.
- [94] K. Yamamoto, K. Takahashi, H. Mizuno, A. Anegawa, K. Ishizaki, H. Fukaki, M. Ohnishi, M. Yamazaki, T. Masujima, T. Mimura, *Proc. Natl. Acad. Sci. USA* **2016**, *113*, 3891–3896.
- [95] L. Zhang, D. P. Foreman, P. A. Grant, B. Shrestha, S. A. Moody, F. Villiers, J. M. Kwake, A. Vertes, *Analyst* **2014**, *139*, 5079–5085.
- [96] L. Zhang, A. Vertes, *Anal. Chem.* **2015**, *87*, 10397–10405.
- [97] N. Pan, W. Rao, N. R. Kothapalli, R. M. Liu, A. W. G. Burgett, Z. B. Yang, *Anal. Chem.* **2014**, *86*, 9376–9380.
- [98] W. Rao, N. Pan, Z. B. Yang, *J. Vis. Exp.* **2016**, 53911.
- [99] H. Y. Zhu, G. C. Zou, N. Wang, M. H. Zhuang, W. Xiong, G. M. Huang, *Proc. Natl. Acad. Sci. USA* **2017**, *114*, 2586–2591.
- [100] H. M. Bergman, I. Lanekoff, *Analyst* **2017**, *142*, 3639–3647.
- [101] B. Shrestha, A. Vertes, *Anal. Chem.* **2009**, *81*, 8265–8271.
- [102] B. Shrestha, J. M. Patt, A. Vertes, *Anal. Chem.* **2011**, *83*, 2947–2955.
- [103] J. A. Stolee, B. Shrestha, G. Mengistu, A. Vertes, *Angew. Chem. Int. Ed.* **2012**, *51*, 10386–10389; *Angew. Chem.* **2012**, *124*, 10532–10535.
- [104] H. Li, B. K. Smith, B. Shrestha, L. Mark, A. Vertes in *Mass Spectrometry Imaging of Small Molecules, Vol. 1203* (Ed.: L. He), Humana Press, New York, **2015**, pp. 117–127.
- [105] J. K. Lee, E. T. Jansson, H. G. Nam, R. N. Zare, *Anal. Chem.* **2016**, *88*, 5453–5461.
- [106] M. Kompauer, S. Heiles, B. Spengler, *Nat. Methods* **2017**, *14*, 90–96.

- [107] D. R. Bandura, V. I. Baranov, O. I. Ornatsky, A. Antonov, R. Kinach, X. D. Lou, S. Pavlov, S. Vorobiev, J. E. Dick, S. D. Tanner, *Anal. Chem.* **2009**, *81*, 6813–6822.
- [108] S. C. Bendall, E. F. Simonds, P. Qiu, E. A. D. Amir, P. O. Krutzik, R. Finck, R. V. Bruggner, R. Melamed, A. Trejo, O. I. Ornatsky, R. S. Balderas, S. K. Plevritis, K. Sachs, D. Pe'er, S. D. Tanner, G. P. Nolan, *Science* **2011**, *332*, 687–696.
- [109] M. H. Spitzer, G. P. Nolan, *Cell* **2016**, *165*, 780–791.
- [110] R. Catena, A. Ozcan, N. Zivanovic, B. Bodenmiller, *Cytometry Part A* **2016**, *89A*, 491–497.
- [111] A. R. Schulz, S. Stanislawiak, S. Baumgart, A. Grutzkau, H. E. Mei, *Cytometry Part A* **2017**, *91A*, 25–33.
- [112] G. K. Behbehani, N. Samusik, Z. B. Bjornson, W. J. Fantl, B. C. Medeiros, G. P. Nolan, *Cancer Discovery* **2015**, *5*, 988–1003.
- [113] M. Wilhelm, J. Schlegl, H. Hahne, A. M. Gholami, M. Lieberenz, M. M. Savitski, E. Ziegler, L. Butzmann, S. Gessulat, H. Marx, T. Mathieson, S. Lemeer, K. Schnatbaum, U. Reimer, H. Wenschuh, M. Mollenhauer, J. Slotta-Huspenina, J. H. Boese, M. Bantscheff, A. Gerstmair, F. Faerber, B. Kuster, *Nature* **2014**, *509*, 582–587.
- [114] A. Koussounadis, S. P. Langdon, I. H. Um, D. J. Harrison, V. A. Smith, *Sci. Rep.* **2015**, *5*, 10775.
- [115] A. L. Bauernfeind, C. C. Babbitt, *BMC Genomics* **2017**, *18*, 322.
- [116] A. P. Frei, F. A. Bava, E. R. Zunder, E. W. Y. Hsieh, S. Y. Chen, G. P. Nolan, P. F. Gherardini, *Nat. Methods* **2016**, *13*, 269–275.
- [117] C. Giesen, H. A. O. Wang, D. Schapiro, N. Zivanovic, A. Jacobs, B. Hattendorf, P. J. Schuffler, D. Grolimund, J. M. Buhmann, S. Brandt, Z. Varga, P. J. Wild, D. Gunther, B. Bodenmiller, *Nat. Methods* **2014**, *11*, 417–422.
- [118] L. L. Sun, M. M. Bertke, M. M. Champion, G. J. Zhu, P. W. Huber, N. J. Dovichi, *Sci. Rep.* **2014**, *4*, 4365.
- [119] L. L. Sun, K. M. Dubiak, E. H. Peuchen, Z. B. Zhang, G. J. Zhu, P. W. Huber, N. J. Dovichi, *Anal. Chem.* **2016**, *88*, 6653–6657.
- [120] P. Nemes, A. M. Knolhoff, S. S. Rubakhin, J. V. Sweedler, *Anal. Chem.* **2011**, *83*, 6810–6817.
- [121] R. M. Onjiko, S. A. Moody, P. Nemes, *Proc. Natl. Acad. Sci. USA* **2015**, *112*, 6545–6550.
- [122] R. M. Onjiko, S. E. Morris, S. A. Moody, P. Nemes, *Analyst* **2016**, *141*, 3648–3656.
- [123] C. Lombard-Banek, S. A. Moody, P. Nemes, *Angew. Chem. Int. Ed.* **2016**, *55*, 2454–2458; *Angew. Chem.* **2016**, *128*, 2500–2504.
- [124] C. Lombard-Banek, S. Reddy, S. A. Moody, P. Nemes, *Mol. Cell. Proteomics* **2016**, *15*, 2756–2768.
- [125] R. M. Onjiko, E. P. Portero, S. A. Moody, P. Nemes, *Anal. Chem.* **2017**, *89*, 7069–7076.
- [126] M. Groessl, S. Graf, R. Knochenmuss, *Analyst* **2015**, *140*, 6904–6911.
- [127] J. Bobrowska, J. Pabijan, J. Wiltowska-Zuber, B. R. Jany, F. Krok, K. Awiuk, J. Rysz, A. Budkowski, M. Lekka, *Anal. Biochem.* **2016**, *511*, 52–60.
- [128] S. Datta, L. Malhotra, R. Dickerson, S. Chaffee, C. K. Sen, S. Roy, *Histol. Histopathol.* **2015**, *30*, 1255–1269.
- [129] S. J. Hoscic, S. K. Murthy, A. N. Koppes, *Anal. Chem.* **2016**, *88*, 354–380.
- [130] S. B. Kodandaramaiah, G. T. Franzesi, B. Y. Chow, E. S. Boyden, C. R. Forest, *Nat. Methods* **2012**, *9*, 585–587.
- [131] L. Li, B. Ouellette, W. A. Stoy, E. J. Garren, T. L. Daigle, C. R. Forest, C. Koch, H. Zeng, *Nat. Commun.* **2017**, *8*, 15604.
- [132] P. Brennecke, S. Anders, J. K. Kim, A. A. Kolodziejczyk, X. W. Zhang, V. Proserpio, B. Baying, V. Benes, S. A. Teichmann, J. C. Marioni, M. G. Heisler, *Nat. Methods* **2013**, *10*, 1093–1095.
- [133] P. V. Kharchenko, L. Silberstein, D. T. Scadden, *Nat. Methods* **2014**, *11*, 740–742.
- [134] Y. Taniguchi, P. J. Choi, G. W. Li, H. Y. Chen, M. Babu, J. Hearn, A. Emili, X. S. Xie, *Science* **2010**, *329*, 533–538.
- [135] O. Gradov, M. Gradova, *Adv. Biochem.* **2015**, *3*, 66–71.

Manuscript received: September 19, 2017

Revised manuscript received: November 27, 2017

Accepted manuscript online: December 7, 2017

Version of record online: March 13, 2018